PACS numbers: 42.55.Px; 42.60.Lh
DOI: 10.1070/QE2002v032n04ABEH002188

Study of characteristics of single-frequency GaAs/AlGaAs semiconductor lasers

V.D.Kurnosov, K.V.Kurnosov, R.V.Chernov

***Abstract*. The characteristics of single-frequency lasers are investigated experimentally and theoretically. It is shown that the model of spectral hole burning with a varying interband relaxation time adequately describes the spectral and modulation characteristics of the laser (taking into account the transport of carriers). The time of carrier capture in a quantum well is 4 ps and the time of their escape is 80 ps.**

Keywords: *single-frequency semiconductor laser, carrier transport, spectral hole burning*.

The simulation of modulation, spectral, and power parameters of semiconductor lasers has become very popular in recent years. Nevertheless, these parameters are analysed separately in the literature. For example, in an analysis of modulation characteristics of a laser, the theoretical and experimental characteristics are correlated by introducing the nonlinearity parameter ε of the gain, which is chosen from the best fit between the theory and the experiment. However, in this case, the spectral characteristics whose behaviour also depends on parameter ε are not considered.

In this work, we carry out a comprehensive analysis of the power, spectral, and modulation characteristics of semiconductor lasers. The characteristics of single-frequency GaAs/AlGaAs ridge lasers with a single quantum well and a Fabry – Perot resonator are investigated experimentally. We used the model of spectral hole burning [1 – 3] for describing the experimental spectral characteristics of the laser. The modulation characteristics of the lasers were calculated using a model taking into account the carrier transport [4, 5].

The lasers investigated by us had an undoped active region; for this reason, we used in our computations the model of radiative transitions with the wave vector selection rules, in which the gain and the rate of spontaneous transitions can be written in the form [6]:

$$g(h\nu)=\sum_{n.i}\int\frac{A_{\rm cv}}{\pi\hbar^2\upsilon_{\rm gr}\rho L_{\rm a}}m_{{\rm r}i}[f_{\rm c}(\mathscr{E}_{{\rm c}ni})-f_{\rm v}(\mathscr{E}_{{\rm v}ni})]\times L(h\nu,E_{\rm cv}){\rm d}E_{\rm cv,} \quad (1)$$

V.D.Kurnosov, K.V.Kurnosov, R.V.Chernov M.F.Stel'makh Polyus Research & Development Institute, ul. Vvedenskogo 3, 117342 Moscow, Russia; e-mail: webeks@comail.ru

Received 20 February 2002
Kvantovaya Elektronika **32** (4) 303 – 307 (2002)
Translated by Ram Wadhwa

$$r_{\rm sp}(h\nu)=\sum_{n.i}\int\frac{A_{\rm cv}}{\pi\hbar^2L_{\rm a}}m_{{\rm r}i}\,f_{\rm c}(\mathscr{E}_{{\rm c}ni})[1-f_{\rm v}(\mathscr{E}_{{\rm v}ni})]\times L(h\nu,E_{\rm cv}){\rm d}E_{\rm cv,} \quad (2)$$

where

$$\mathscr{E}_{{\rm c}ni}=E_{\rm c0}+(m_{{\rm r}i}/m_{\rm c})(E_{\rm cv}-E_{\rm g})+(m_{{\rm r}i}/m_{{\rm v}i{\rm t}})E_{cn}-(m_{{\rm r}i}/m_{\rm c})E_{vin};$$
$$\mathscr{E}_{{\rm v}ni}=E_{\rm v0}-(m_{{\rm r}i}/m_{{\rm v}i{\rm t}})(E_{\rm cv}-E_{\rm g})+(m_{{\rm r}i}/m_{{\rm v}i{\rm t}})E_{cn}-(m_{{\rm r}i}/m_{\rm c})E_{vin}; \quad (3)$$

$h\nu$ is the photon energy; $A_{\rm cv}$ is the Einstein coefficient; ρ is the density of electromagnetic field modes in the crystal; $L_{\rm a}$ is the thickness of the active region; $m_{\rm c}$ is the effective electron mass; $m_{{\rm v}i{\rm t}}$ are the transverse components of the effective masses of light and heavy holes; $m_{{\rm r}i}=m_{\rm c}m_{{\rm v}i{\rm t}}/(m_{\rm c}+m_{{\rm v}i{\rm t}})$ is the reduced mass taking into account the corresponding holes; $\upsilon_{\rm gr}$ is the group velocity of light; and $f_{\rm c}(\mathscr{E}_{{\rm c}ni})$ and $f_{\rm v}(\mathscr{E}_{{\rm v}ni})$ are the Fermi – Dirac functions (subscript $i={\rm h,l}$ corresponds to heavy and light holes, respectively, and n is the number of the subband). The lower integration limit in Eqns (1) and (2) is $h\nu_{ni}=E_{\rm g}+E_{cn}+E_{vin}$, which corresponds to the energy of initial transitions for subbands with the number n. Here, $E_{\rm g}=E_{\rm c0}-E_{\rm v0}$; $E_{\rm c0}$ is the bottom of the conduction band; $E_{\rm v0}$ is the top of the valence band; E_{cn} are the ground states of the electron subbands; and E_{vin} are the ground states of the hole subbands, which are determined by the longitudinal components of the effective masses $m_{{\rm v}i{\rm l}}$ of holes. The upper integration limit is bounded by the height of potential barriers.

The broadening of an emission line is described by the Lorentzian

$$L(h\nu-E_{\rm cv})=\frac{1}{\pi}\frac{\Gamma_{\rm cv}}{(h\nu-E_{\rm cv})^2+\Gamma_{\rm cv}^2}, \quad (4)$$

where $\Gamma_{\rm cv}=\hbar/\tau_{\rm in}$; $\tau_{\rm in}$ is the intraband relaxation time of charge carriers; and $2\Gamma_{\rm cv}$ is the emission line width.

The averaged square of the matrix element of band – band transitions appearing in $A_{\rm cv}$ is defined as $|{\rm M}|^2=\alpha_{ni}|{\rm M_{cv}}|^2$, where $|{\rm M_{cv}}|^2=3.38m_0E_{\rm g}$ [7]. The coefficient α_{ni} characterising the 'polarisation' dispersion for the TE mode and for transitions to the levels of heavy and light holes is determined by the expression [6, 8]

$$\alpha_{nh} = \frac{3}{4}(1+\cos^2\theta), \quad \alpha_{nl} = \frac{1}{4}(5-3\cos^2\theta), \tag{5}$$

where $\cos^2\theta = (E_{cn}+E_{vin})/(E_{cv}-E_g)$ and θ is the angle between the size-quantisation axis $<100>$ and the wave vector for holes.

The total rate of spontaneous recombination is

$$R_{sp} = \int r_{sp}(h\nu)\mathrm{d}h\nu = \frac{n_1}{\tau_n}, \tag{6}$$

where $r_{sp}(h\nu)$ is defined by expression (2); τ_n is the time constant of radiative recombination, and

$$n_1 = \int_{E_{c0}+E_{c1}}^{E_b} \rho_c(E) f_c(E)\mathrm{d}E \tag{7}$$

is the carrier density in the active region of the laser. The Fermi quasilevels F_c and F_v in the conduction and valence bands, respectively, are related through the electroneutrality equation [9]: $L_a(n_1-p_1)+L_b(n_2-p_2)=0$, where $n_1(F_c)$ and $p_1(F_v)$ are the concentrations of electrons and holes in the active region, $n_2(F_c)$ and $p_2(F_v)$ are the concentrations of carriers in the waveguide layer, and L_b is the thickness of the waveguide layer.

In our calculations, we took into account the narrowing of the band gap in $GaAs/Al_xGa_{1-x}As$ in the active region upon pumping the laser structure by a current:

$$E_g = 1.424 + 1.247x - 1.6\times10^{-8}(n_1^{1/3}+p_1^{1/3}). \tag{8}$$

In the steady-state case, the volume densities S_m of photons in the mth mode with energy E_m are described by the expression [1–3]

$$v_{gr}\left[\Gamma_a g(E_m) - \varepsilon_m S_m - \sum_{q\neq m} D_q S_q - \alpha\right] S_m + \beta R_{sp} = 0, \tag{9}$$

where Γ_a is the coefficient of optical confinement in the active region and β is the coefficient taking into account the contribution of spontaneous emission to the lasing mode.

The coefficients ε_m and D_q have the form [1–3]

$$\varepsilon_m = \frac{9}{4}\frac{E_m\Gamma_a\alpha}{\varepsilon^{(0)}n_{gr}^2}\left(\frac{\tau_{in}}{\hbar}\right)^2\langle R_{cv}\rangle^2,$$
$$D_q = \frac{4}{3}\frac{\varepsilon_m}{1+(\tau_{in}\omega_q/\lambda_q)^2(\lambda_m-\lambda_q)^2}, \tag{10}$$

where $\langle R_{cv}\rangle^2$ is the dipole moment; n_{gr} is the group refractive index; $\varepsilon^{(0)}$ is the permittivity; λ_m and λ_q are wavelengths of modes with numbers m and q. Laser losses are given by the expression

$$\alpha = \alpha_0 + \frac{1}{L}\ln\frac{1}{R}, \tag{11}$$

where α_0 are nonresonance losses; L is the laser resonator length; and R is the reflectivity of mirrors.

The total optical power is determined by the expression

$$P = \sum P_m = \frac{1}{2}h\nu\frac{V_a}{L}\frac{c}{n_{gr}}\ln\frac{1}{R}\sum S_m, \tag{12}$$

where P_m is the optical power of radiation in the mth mode and V_a is the volume of the active region.

The calculations were made using the following parameters: $m_c = 0.067m_0$, $m_{vhl} = 0.34m_0$, $m_{vll} = 0.094m_0$, $m_{vlt} = 0.20m_0$ [6], T = 293 K, $x_a = 0$, $x_b = 0.3$, $L_a = 80$ Å, $L_b = 200$ nm, $L = 400$ μm, $V_a = 1.6\times10^{-11}$ cm^{-3}, $\Gamma_a = 0.024$, $\langle R_{cv}\rangle^2 = 4.6\times10^{-53}$ C^2 cm^2, $\alpha_0 = 20$ cm^{-1}, and $\beta = 4.7\times10^{-4}$.

Fig. 1 shows the theoretical and experimental spectral characteristics of the laser for the intraband relaxation times $\tau_{in} = 10^{-13}$ s and 1.5×10^{-13} s. One can see that the spectral characteristics calculated from expression (9) for $\tau_{in} = 10^{-13}$ s [curve (*2′*)] and $\tau_{in} = 1.5$ s [curve (*2″*)] are smoothly decreasing functions, while experiments indicate that the dependence exhibits a slow increase for a power higher than 4–5 mW. For matching the theory and experiment, it was assumed in [10] that τ_{in} is a function of radiation power:

$$\tau_{in} = \frac{\tau_{in}^{(0)}}{1+P/P_n}, \tag{13}$$

where $\tau_{in}^{(0)} = 2\times10^{-13}$ s and $P_n = 5$ mW are determined from the best fit between the theoretical and experimental results. The spectral characteristics calculated taking into account expression (13) are presented by curves (*1*) and (*2*) in Fig. 1.

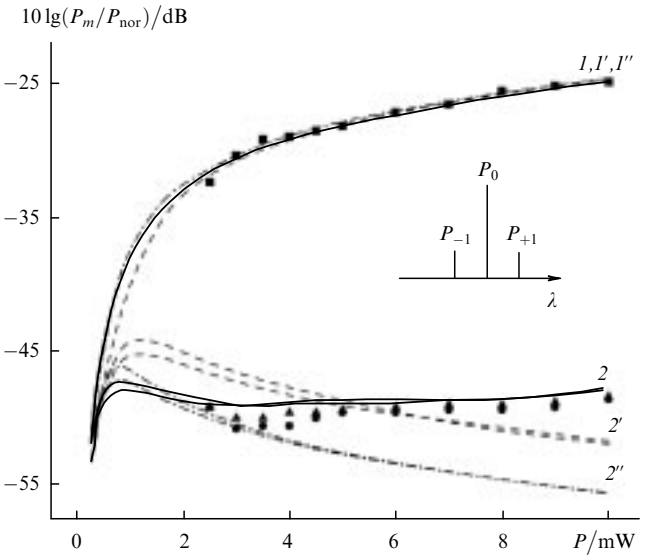

Figure 1. Radiation power in the lasing ($m=0$) mode $10\lg(P_0/P_{nor})$ (curves *1*, *1′*, *1″*) and in adjacent modes ($m=\pm1$) $10\lg(P_{\pm1}/P_{nor})$ (*2*, *2′*, *2″*), normalised to the optical radiation power P_{nor} (determined from the experimental conditions) as functions of the total output radiation power of a semiconductor laser. Calculations were made for τ_{in} defined by expression (13) (*1*, *2*) and for $\tau_{in} = 10^{-13}$ s (*1′*, *2′*) and 1.5×10^{-13} s (*1″*, *2″*). Experimental dependences: $m=0$ (■), –1 (▲), +1 (●).

Fig. 2 shows the experimental and theoretical emission spectra of a laser diode for a radiation power of 5 mW. One can see that the theoretical and experimental curves coincide satisfactorily not only for the zeroth mode, but also for adjacent modes.

Fig. 3 presents the experimental and theoretical light–current characteristics for constant intraband relaxation times $\tau_{in} = 10^{-13}$ and 1.5×10^{-13} s, as well as for the

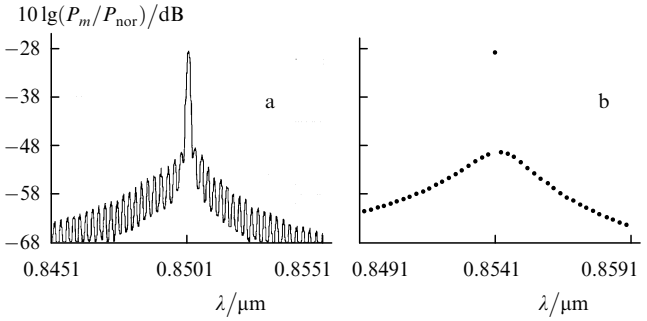

Figure 2. Experimental (a) and theoretical (b) emission spectra of a laser diode. The spectra correspond to the optical radiation power $P = 5.0$ mW.

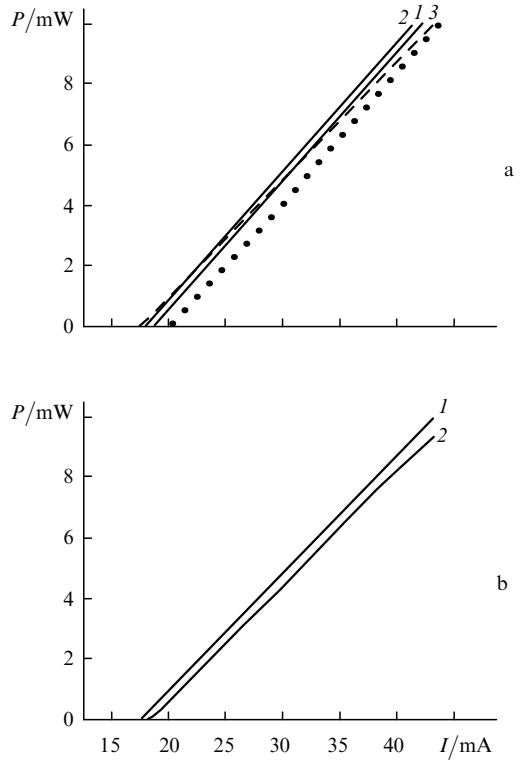

Figure 3. (a) Light–current characteristics of the total radiation power for $\tau_{\rm in} = 10^{-13}$ s (curve *1*), 1.5×10^{-13} s (curve *2*), and $\tau_{\rm in}$ defined by expression (13) (curve *3*), and (b) the dependence of the total radiation power (*1*) and radiation power in the zeroth mode (*2*) for $\tau_{\rm in}$ defined by expression (13); dark circles correspond to experimental results.

varying time $\tau_{\rm in}$ defined by expression (13). A comparison of Figs 1 and 3 shows that the inclusion of different intraband relaxation times strongly affects the spectral characteristics of a semiconducting laser, but changes its light–current characteristics only slightly. Calculations show (see Fig. 3b) that virtually the entire laser radiation power is concentrated in the zeroth mode; consequently, an analysis of the modulation characteristics can be carried out using the single-frequency approximation.

The modulation characteristics were calculated using the 3N model [4, 5]:

$$\frac{{\rm d}n_3}{{\rm d}t} = D\frac{{\rm d}^2 n_3}{{\rm d}z^2} - R_3(n_3), \tag{14}$$

$$\frac{{\rm d}n_2}{{\rm d}t} = \frac{I_{n_2}}{eV_{\rm a}} - \frac{I_{\rm net}}{eV_{\rm a}} - R_2(n_2), \tag{15}$$

$$\frac{{\rm d}n_1}{{\rm d}t} = \frac{I_{\rm net}}{eV_{\rm a}} - R_1(n_1) - \Gamma_{\rm a} v_{\rm gr} GS, \tag{16}$$

$$\frac{{\rm d}S}{{\rm d}t} = \Gamma_{\rm a} v_{\rm gr} GS - \frac{S}{\tau_{\rm p}}, \tag{17}$$

where $n_1, n_2, n_3, R_1(n_1), R_2(n_2), R_3(n_3)$ are the densities of charge carriers and their recombination rates in the active region, the waveguide layer above the active region, and in the waveguide layers, respectively (see Fig. 3 from [4]; the 3N model); S, G, and $\tau_{\rm p}$ are the density of photons in the resonator, the gain, and the lifetime of photons, respectively; $I_{\rm net}$ is the current determined by the capture and escape of carriers from a quantum well; and D is the ambipolar diffusion coefficient.

In the small-signal analysis, the following linearisation is used:

$$G(n_1, S) = G(n_{10}, S_0) + \left.\frac{\partial G}{\partial n_1}\right|_0 \Delta n_1 + \left.\frac{\partial G}{\partial S}\right|_0 \Delta S$$

$$\equiv G_0 + g\Delta n_1 + \xi \Delta S, \tag{18}$$

where

$$\xi \equiv \left.\frac{\partial G}{\partial S}\right|_0 = -\frac{G_0 \varepsilon_{\rm sh}}{1 + \varepsilon_{\rm sh} S_0};\ g = \frac{g_0}{1 + \varepsilon_{\rm sh} S_0};\ \varepsilon_{\rm sh} = \frac{\varepsilon_0}{\alpha};$$

$$g_0 = \left.\frac{\partial G^{(1)}}{\partial n_1}\right|_0$$

is the differential gain for $G = G^{(1)}(n)/(1 + \varepsilon_{\rm sh} S)$. In calculations, a linear approximation of the gain maximum presented by the straight line (*3*) in Fig. 4 is used for $G^{(1)}(n)$. Curves (*1*) and (*1′*) are the dependences of maximum of the gain on the carrier density calculated by formula (1) for $\tau_{\rm in} = 10^{-13}$ and 1.5×10^{-13} s, respectively. Curve (*2*) is a logarithmic approximation of the gain. Although the logarithmic dependence approximates curve (*1*) better, we will use in subsequent calculations the more traditional linear approximation [curve (*3*)]; in this

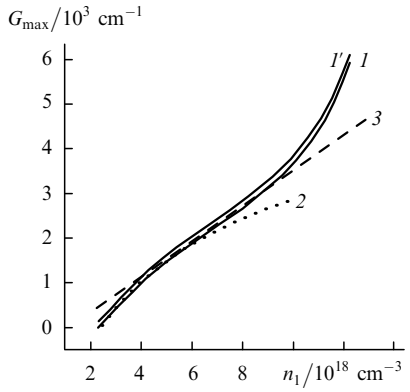

Figure 4. Dependence of the maximum gain on the carrier density in the active region, calculated according to the model of radiative transitions with selection rules for the wave vector for $\tau_{\rm in} = 10^{-13}$ s (*1*) and 1.5×10^{-13} s (*1′*); curves *2* and *3* correspond to the logarithmic and linear approximations, respectively.

case, $G^{(1)}(n_1) = g_0(n_1 - n_0)$, where $g_0 = 4 \times 10^{-16}$ cm^2 is independent of the intraband relaxation time for charge carriers.

The current I_{net} is determined by the expression [4]

$$I_{\text{net}}(n_2, n_1) = I_{\text{net}}(n_{20}, n_{10}) + \left.\frac{\partial I_{\text{net}}}{\partial n_1}\right|_0 \Delta n_1 + \left.\frac{\partial I_{\text{net}}}{\partial n_2}\right|_0 \Delta n_2$$

$$\equiv eV_{\text{a}}\left(\frac{n_{20}}{\tau_{\text{c0}}} - \frac{n_{10}}{\tau_{\text{es0}}} + \frac{\Delta n_2}{\tau_{\text{c}}} - \frac{\Delta n_1}{\tau_{\text{es}}}\right), \tag{19}$$

where $\tau_{\text{c0}}, \tau_{\text{es0}}, \tau_{\text{c}}$, and τ_{es} are the local time constants of capture and escape of carriers for a direct current and a variable signal.

In the case of direct modulation of laser radiation, the pump current can be written in the form $I = I_0 + \tilde{I}e^{j\omega t}$ (I_0 and $\tilde{I}$ are the constant and alternating components of the pump current and $\omega = 2\pi f$), while the densities of charge carriers and the density of photons can be written as $x = x_0 + \tilde{x}e^{j\omega t}$, where $\tilde{x} = n_1, n_2, n_3, S$.

The modulation characteristic has the following form [4]:

$$M = 10 \lg\left[\frac{1}{1 + \omega^2\tau_{\text{ce}}^2} \frac{\omega_0^4}{(\omega_0^2 - \omega^2)^2 + \omega^2\mu^2}\right], \tag{20}$$

where

$$\omega_0^2 = \frac{\Gamma_{\text{a}} v_{\text{gr}} g_0 S_0}{(1 + Rr)(1 + \varepsilon_{\text{sh}} S_0)\tau_{\text{p}}} \tag{21}$$

is the resonance frequency;

$$\mu = \frac{1}{(1 + Rr)\tau_{n_1}} + \frac{Rr}{1 + Rr}\left(\frac{1}{r\tau_{n_2}} + \frac{r - 1}{r\tau_{n_3}}\right)$$

$$+ \omega_0^2\left[\tau_{\text{p}} + \frac{(\varepsilon_{\text{sh}} + \varepsilon_{\text{ce}})(1 + Rr)}{\Gamma_{\text{a}} v_{\text{gr}} g_0}\right] \tag{22}$$

is the damping decrement;

$$\tau_{\text{ce}} = r\tau_{\text{c}} + \tau_{\text{D}};\ R = \frac{\tau_{\text{c}}}{\tau_{\text{es}}};\ r = \frac{L_{\text{b}}}{L_{\text{a}}};\ \varepsilon_{\text{ce}} = \frac{Rr\Gamma_{\text{a}} v_{\text{gr}} g_0}{(1 + Rr)^2}\tau_{\text{ce}};$$

$$\tau_{\text{D}} = \frac{(L_{\text{b}} - L_{\text{a}})^2}{8D};$$

ε_0 is described by expression (10) for $m = 0$; and α are the losses (11).

Calculations show that the carrier density in the waveguide layers is much smaller than in the active region of the laser, and we can assume that $\tau_{n_2}, \tau_{n_3} \gg \tau_{n_1}$; consequently, the middle term in expression (22) can be neglected. The modulation characteristics were calculated for $\tau_{n_1} = 0.8 \times 10^{-9}$ s [taking into account the radiative (6) and nonradiative recombination processes] and $\tau_{\text{D}} = 5 \times 10^{-12}$ s.

Fig. 5 shows the modulation characteristics calculated for a radiation power of 1, 2, and 3 mW. By varying the values of τ_{c} and R and using expressions (20)–(22) for a constant time of intraband relaxation of charge carriers $\tau_{\text{in}} = 10^{-13}$ s [see curve (*2′*) in Fig. 1], we obtained the best fit between the theory and experiment. The results are presented in Fig. 5 [curves (*1*)] for $\tau_{\text{c}} = 4 \times 10^{-12}$ s and $R = 0.05$.

Curves (*2*) in Fig. 5 present the modulation characteristics for the model in which the time τ_{in} was determined by the expression (13) [see curve (*2*) in Fig. 1] for the same

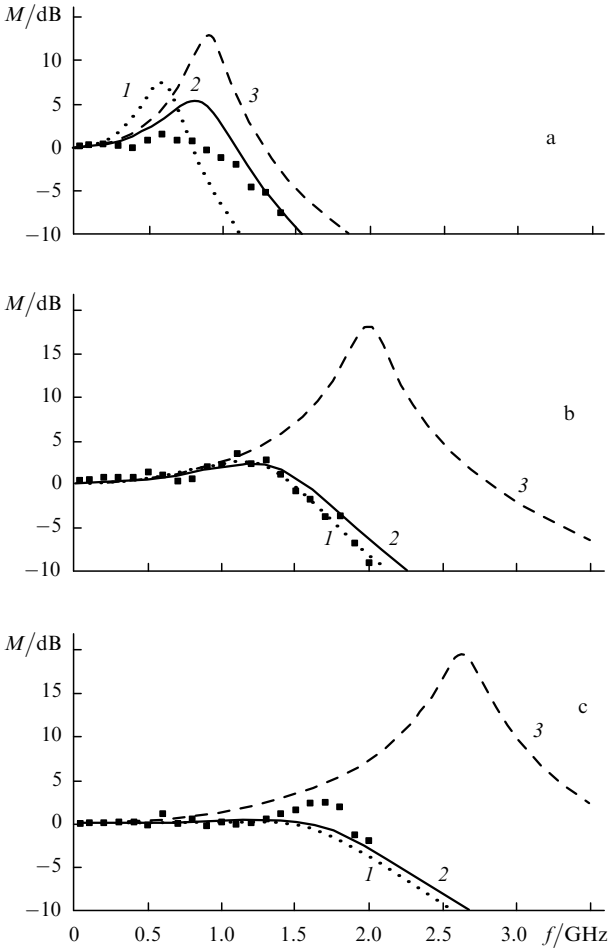

Figure 5. Modulation characteristics calculated for power $P =$ (a) 1, (b) 2, and (c) 3 mW. Curves *1* are calculated for a constant intraband relaxation time $\tau_{\text{in}} = 10^{-13}$ s, curves *2* are calculated in the model with τ_{in}, defined by expression (13), and curves *3* correspond to the model neglecting carrier transport; squares show the experimental results.

values of τ_{c} and R. The coefficient ε_m (10) is a function of τ_{in}^2; consequently, the gain has the form

$$G = G^{(1)}(n_1)\left[1 + \frac{\varepsilon_{\text{sh}} S}{1 + S/S_{\text{n}}}\right]^{-1}, \tag{23}$$

where S_{n} is the density of photons corresponding to the radiation power $P_{\text{n}} = 5$ mW.

The resonance frequency is given by

$$\omega_0^2 = \Gamma_{\text{a}} v_{\text{gr}} g_0 S_0 (1 + Rr)^{-1}\left[1 + \frac{\varepsilon_{\text{sh}} S_0}{1 + S_0/S_{\text{n}}}\right]^{-1}\tau_{\text{p}}^{-1} \tag{24}$$

and the damping decrement is

$$\mu = \frac{1}{(1 + Rr)\tau_{n_1}} + \omega_0^2\left\{\tau_{\text{p}} + \frac{[\varepsilon_{\text{sh}}(S_0) + \varepsilon_{\text{ce}}](1 + Rr)}{\Gamma_{\text{a}} v_{\text{gr}} g_0}\right\}, \tag{25}$$

where

$$\varepsilon_{\text{sh}}(S_0) = \frac{\varepsilon_{\text{sh}}(1 - S_0/S_{\text{n}})}{(1 + S_0/S_{\text{n}})^3}.$$

A comparison of the theoretical curves (*2*) in Fig. 5 with experimental curves shows their satisfactory coincidence. Thus, we can assume that the local capture time of carriers in a quantum well is $\tau_c \approx 4 \times 10^{-12}$ s, while the escape time is $\tau_{es} \approx 80 \times 10^{-12}$ s; $R = \tau_c/\tau_{es} = 0.05$. For comparison, Fig. 5 shows the modulation characteristics of the laser neglecting the transport of charge carriers (curves *3*).

Fig. 6a shows the modulation characteristics of the laser for a fixed radiation power $P = 2$ mW for different times τ_c of carrier capture in a quantum well and a fixed time of charge carrier escape $\tau_{es} = 80 \times 10^{-12}$ s, while Fig. 6b, on the contrary, shows the same dependences for the fixed $\tau_c = 4 \times 10^{-12}$ s, but for different values of τ_{es}. One can see that to increase the laser response, it is necessary to decrease the capture time and increase the escape time of charge carriers from the quantum well.

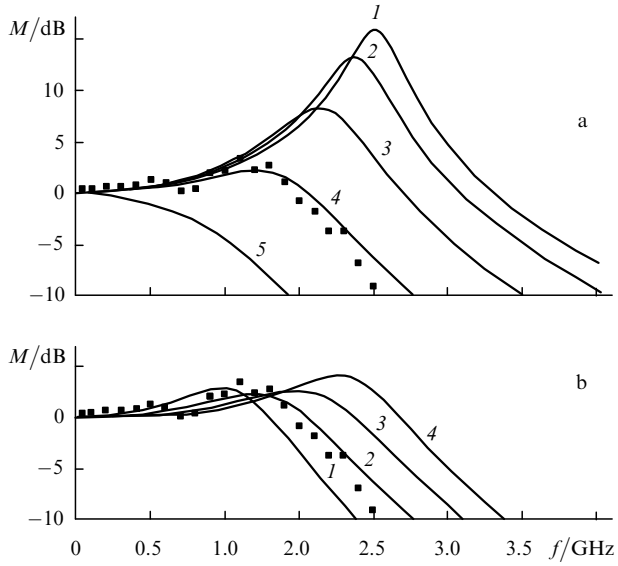

Figure 6. Modulation characteristics calculated for a radiation power $P = 2$ mW, $\tau_{in}(0) = 2 \times 10^{-13}$ s, and $\tau_D = 5 \times 10^{-12}$ s for $\tau_{es} = 80 \times 10^{-12}$ s and $\tau_c = 0.5$, 1, 2, 4, and 8 ps [curves (*1–5*), respectively] (a), as well as for $\tau_c = 4 \times 10^{-12}$ s and $\tau_{es} = 40$, 80, 160, and 320 ps [curves (*1–4*), respectively] (b); squares correspond to experiment.

Thus, the model taking into account the carrier transport describes satisfactorily the modulation characteristics, while the model of spectral hole burning with a varying intraband relaxation time adequately describes the spectral and modulation characteristics of the laser.

References

1. Suemutsu Y., Adams A.R. *Handbook of Semiconductor Lasers and Photonic Integrated Circuits* (London, Chapman and Hall, 1994).
2. Yamada M., Suematsu Y. *J. Appl. Phys.,* **52**, 2653 (1981).
3. Asada M., Suematsu Y. *IEEE J. Quantum Electron.*, **QE-21**, 434 (1985).
4. Tsai C.Y., Lo Y.H., Spencer R.M., Eastman L.F., Tsai C.Y. *IEEE J. Select. Topic in Quantum Electron.*, **1**, 316 (1995).
5. Kan S.C., Vassilovski D., Wu T.C., Lau K.Y. *Appl. Phys. Lett.*, **62**, 2307 (1993).
6. Kononenko V.K., Manak I.S., Furunzhiev E.R. *Zh. Prikl. Spektrosk.*, **64**, 797 (1997).
7. Yan R.H., Corrine S.W., Coldren L.A., Suemune I. *IEEE J. Quantum Electron.*, **QE-26**, 213 (1990).
8. Yamanishi M., in *Fizika poluprodnikovykh lazerov* (Physics of Semiconductor Lasers) (Moscow: Mir, 1989).
9. Wilcox J.Z., Ou S., Yang J.J., Jansen M., Peterson G.L. *Appl. Phys. Lett.*, **55**, 825 (1989).
10. Kurnosov V.D., Kurnosov K.V. *Zh. Prikl. Spektrosk.*, **67**, 535 (2000).